

DTIC FILE COPY

①

NASA Contractor Report 181997

ICASE Report No. 90-15

AD-A227 100

ICASE

THE ANALYSIS AND SIMULATION OF
COMPRESSIBLE TURBULENCE

Gordon Erlebacher
M. Y. Hussaini
H. O. Kreiss
S. Sarkar

Contract No. NAS1-18605
February 1990

Institute for Computer Applications in Science and Engineering
NASA Langley Research Center
Hampton, Virginia 23665-5225

Operated by the Universities Space Research Association

DTIC
ELECTE
OCT 03 1990
S E D
Ca

NASA

National Aeronautics and
Space Administration

Langley Research Center
Hampton, Virginia 23665-5225

DISTRIBUTION STATEMENT A

Approved for public release;
Distribution Unlimited

90

~~90 03 19 014~~

THE ANALYSIS AND SIMULATION OF COMPRESSIBLE TURBULENCE¹

Gordon Erlebacher

*Institute for Computer Applications in Science and Engineering
NASA Langley Research Center, Hampton, VA 23665*

M. Y. Hussaini

*Institute for Computer Applications in Science and Engineering
NASA Langley Research Center, Hampton, VA 23665*

H. O. Kreiss

*University of California at Los Angeles
Los Angeles, CA 90024*

S. Sarkar

*Institute for Computer Applications in Science and Engineering
NASA Langley Research Center, Hampton, VA 23665*

Accession For	
AMS	GRA&I <input checked="" type="checkbox"/>
INFO TAB	<input type="checkbox"/>
Announced	<input type="checkbox"/>
Justification	
By _____	
Distribution/	
Availability Codes	
Dist	Avail and/or Special
A-1	



ABSTRACT

This paper considers compressible turbulent flows at low turbulent Mach numbers. Contrary to the general belief that such flows are almost incompressible, (i.e. the divergence of the velocity field remains small for all times), it is shown that even if the divergence of the initial velocity field is negligibly small, it can grow rapidly on a non-dimensional time scale which is the inverse of the fluctuating Mach number. An asymptotic theory which enables one to obtain a description of the flow in terms of its divergence-free and vorticity-free components has been developed to solve the initial-value problem. As a result, the various types of low Mach number turbulent regimes have been classified with respect to the initial conditions. Formulae are derived that accurately predict the level of compressibility after the initial transients have disappeared. These results are verified by extensive direct numerical simulations of isotropic turbulence.

¹Research was supported by the National Aeronautics and Space Administration under NASA Contract No. NAS1-18605 while all of the authors were in residence at the Institute for Computer Applications in Science and Engineering (ICASE), NASA Langley Research Center, Hampton, VA 23665.

I. Introduction

Turbulence is the most common state of fluid motion. It is an all pervasive ubiquitous phenomenon present in, to cite a few instances, weather patterns, ocean currents, high-temperature plasmas, astrophysical jets, and combustion. Despite the best theoretical and experimental attempts of more than a century, and more recent computational approaches, turbulence remains to be one of the great unsolved problems of fundamental physics, and poses a grand challenge to any type of scientific investigation.

There has of course been some progress in our understanding of turbulence in low-speed flows which are essentially incompressible (see Dwoyer, Hussaini and Voigt 1984). There have also been a few attempts at predicting the effect of compressibility on some known results of incompressible turbulence such as the Kolmogorov spectrum (Zakharov and Sagdeev 1970, Kadomtsev and Petvishvili 1973, Moiseev, Sagdeev, Tur and Yanovskii 1977, and L'vov and Mikhailov 1978). The majority of work in compressible turbulence focuses naturally on the linear regime, owing to the inherent difficulty of treating nonlinearities which now involve variable density as well. Moyal (1952) appears to be the first one to look at spectra of homogeneous isotropic turbulence in compressible fluids. He decomposed the velocity field in the spectral space into a longitudinal component (random noise) and a transverse (eddy turbulence) component. This is in fact equivalent to a Helmholtz decomposition (gradient of a scalar and curl of a vector) in physical space. The longitudinal component in physical space is variously known as the acoustic component or compression turbulence; the transverse component is also termed the incompressible component, the solenoidal component or shear turbulence. A broad conclusion of his work was that the interaction between these two components is exclusively due to the nonlinear terms, and such interactions are the strongest at high levels of turbulence and at high values of Reynolds number. The properties of sound emitted in the far field by eddy turbulence were studied by Lighthill (1952, 1954, 1956). His formula for sound emission is found in laboratory experiments to remain valid far beyond the linear regime. Kovasznay (1957) proposed a decomposition of compressible turbulence into three modes – the vorticity mode, the entropy mode and the acoustic mode – and showed how to determine their levels and correlations from mass flow and stagnation temperature fluctuations measured by a hot-wire anemometer. Chu and Kovasznay (1958) have outlined a consistent successive approximation procedure in terms of an amplitude parameter, and have provided explicit formulae for second-order interactions among these three modes. They provide no explicit solutions since their main purpose was to provide a consistent framework to assess the nonlinear interactions in the experimental data. Tatsumi and Tokunaga (1974) and Tokunaga and Tatsumi (1975) study the interactions of weakly nonlinear disturbances such as compression waves, expansion waves and contact discontinuities using a reductive perturbation method due to Taniuti and Wei (1968). The key result is that the interaction between waves

of different families of characteristics leads to alterations in their amplitudes, phase velocities and propagation directions, whereas the interaction between waves of the same family of characteristics causes merger or coalescence. They further inferred that the statistical properties of two-dimensional shock turbulence are similar to those of one-dimensional shock turbulence which in turn are identical to those of Burgers turbulence. More recently, in a preliminary study of return to isotropy in a compressible flow, Lumley (1989) has provided some orders of magnitude estimates in terms of Mach number and Reynolds number. An excellent review of the published literature on compressible turbulence up to 1967 may be found in Monin and Yaglom (1967).

The computational approach to turbulence is based on the Navier-Stokes equations. The first attempt to solve numerically the equations of motion for compressible homogeneous turbulence is due to Feiereisen, Reynolds and Ferziger (1981). They assumed the divergence of the initial flow field and its time-derivative to be both zero. It was therefore not surprising that their results for isotropic compressible turbulence did not show any departure from the corresponding incompressible data. Recently, Passot and Pouquet (1986) have carried out numerical simulations of two-dimensional homogeneous compressible turbulent flows. They show that the behavior of the flow beyond an initial turbulent Mach number of 0.3 differs sharply from the lower Mach number cases which are characterized by the absence of shocks.

In the present paper, we develop an asymptotic theory (with turbulent Mach number as a small parameter) to solve the compressible Navier-Stokes equations. The problem is set up as an initial-value problem to study the influence of initial conditions on the subsequent turbulence structure and its dynamical evolution. Explicit relationships between the initial turbulent Mach number, pressure and velocity fluctuation levels are derived which are valid after the initial time transients have disappeared. Direct numerical simulations of two-dimensional isotropic compressible turbulence are performed to validate the results.

II. Theoretical Analysis

A. Problem Formulation

The compressible Navier Stokes equations are, in non-dimensional variables,

$$\begin{aligned}
 \frac{\partial \rho}{\partial t} + \nabla \cdot (\rho \mathbf{u}) &= 0, \\
 \frac{\partial (\rho \mathbf{u})}{\partial t} + \nabla \cdot (\rho \mathbf{u} \mathbf{u}) &= -\frac{1}{\gamma M_R^2} \nabla P + \frac{1}{Re} \nabla \cdot \vec{\sigma}, \\
 \frac{\partial P}{\partial t} + \mathbf{u} \cdot \nabla P + \gamma P \nabla \cdot \mathbf{u} &= \frac{\gamma}{Re Pr} \nabla \cdot \kappa \nabla T + \frac{\gamma(\gamma-1)M_R^2}{Re} \Phi,
 \end{aligned} \tag{1}$$

where

$$\vec{\sigma} = 2\mu \left[\frac{1}{2}(\nabla\mathbf{u} + \nabla\mathbf{u}^T) - \frac{1}{3}(\nabla\cdot\mathbf{u})\vec{\mathbf{I}} \right] \quad (2)$$

is the viscous stress tensor (with bulk viscosity assumed zero), $\vec{\mathbf{I}}$ is the identity tensor, and

$$\Phi = \frac{1}{2}(\nabla\mathbf{u} + \nabla\mathbf{u}^T) : \vec{\sigma} \quad (3)$$

is the viscous dissipation function. The equation of state is

$$P = \rho T. \quad (4)$$

The density, velocity, temperature and pressure are respectively

$$\begin{aligned} \rho &= \frac{\rho^*}{\rho_R}, \\ \mathbf{u} &= \frac{\mathbf{u}^*}{U_R}, \\ T &= \frac{T^*}{T_R}, \\ P &= \frac{p^*}{R_g \rho_R T_R}. \end{aligned}$$

where the dimensional reference values are denoted by the subscript R and R_g is the universal gas constant. Dimensional variables have an asterisk superscript. Distance and time are scaled respectively with respect to L_R and $t_R = L_R/U_R$. In the text, \mathbf{x} refers to the cartesian position vector.

The Prandtl number $Pr = (\mu_R C_p)/\kappa_R$, the Reynolds number $Re = (\rho_R U_R L_R)/\mu_R$; γ is the ratio of specific heats. Viscosity and conductivity are denoted by μ and κ respectively and are scaled with respect to μ_R and κ_R .

The reference Mach number

$$M_R = \frac{U_R}{\sqrt{\gamma R_g T_R}} \quad (5)$$

is related to the time-dependent turbulent Mach number

$$\begin{aligned} M_t &= \sqrt{\left\langle \frac{\mathbf{u}^{*2}}{\gamma R_g T^*} \right\rangle} \\ &= M_R \sqrt{\left\langle \frac{u^2}{T} \right\rangle}. \end{aligned} \quad (6)$$

The objectives of the following analysis is first to classify the various types of equilibrium turbulent regimes (distinguished by the presence or absence of shocks and

also by the fraction of the total kinetic energy solely due to compressibility effects), and second, to predict the range of initial conditions that leads to each one. The effect of viscosity is felt either on a viscous time scale (much greater than the acoustic time scale), or during the formation of shocks. In the latter case, viscosity serves to prevent the formation of singularities. Although there is a distinct possibility that shocks will form as a result of certain types of initial conditions, viscosity does not help initiate the processes (wave steepening) which eventually lead to shocks. Rather, the viscosity diffuses the sharp gradients to generate shocks of finite thickness. The above considerations lead us to neglect all viscous effects in the theoretical formulation of the full viscous, Navier-Stokes equations. This assumption will be verified a posteriori by the direct numerical simulations.

In the following analysis, the turbulent Mach number is assumed to be very much less than unity, so that the sound velocity is much greater than the flow velocity. Under these circumstances, the acoustic time scale is much less than the convective time scale, which in turn is much less than the viscous time scale (if the Reynolds number is sufficiently large). As will be shown later, the different regimes emerge on the acoustic time scale, during which time any inconsistency in the acoustic component of the flow is washed away. In other words, time boundary layers only extend over a time period of $O(M_R)$.

Dropping the viscous and heat conduction terms, Eqs. (1) become (in nonconservative form)

$$\begin{aligned}\frac{\partial \rho}{\partial t} + \mathbf{u} \cdot \nabla \rho + \rho \nabla \cdot \mathbf{u} &= 0, \\ \rho \left(\frac{\partial \mathbf{u}}{\partial t} + \mathbf{u} \cdot \nabla \mathbf{u} \right) + \frac{1}{\gamma M_R^2} \nabla P &= 0, \\ \frac{\partial P}{\partial t} + \mathbf{u} \cdot \nabla P &= -\gamma P \nabla \cdot \mathbf{u}.\end{aligned}\tag{7}$$

The initial conditions are arbitrary with the restriction that both M_R and the root mean square (rms) pressure, $\|p(\mathbf{x}, 0)\|$, be much less than unity. For the remainder of this analysis, we assume that for homogeneous turbulent flows, the maximum norm and the L_2 norm are of the same order of magnitude.

B. Asymptotic Analysis

The system of equations (7) is now investigated by an asymptotic analysis which assumes $M_R \ll 1$. The pressure P is decomposed into a mean and a fluctuating component:

$$P = 1 + p,\tag{8}$$

where

$$\|p\| \ll 1.\tag{9}$$

For simplicity, we neglect any consideration of the entropy mode and assume the homentropic condition

$$P = \rho^\gamma. \quad (10)$$

The density is expanded in powers of p according to

$$\rho = 1 + \gamma^{-1}p + O(\|p\|^2). \quad (11)$$

Using the expansions (8) for pressure and (11) for density, Eqs. (7) become (to first order in $\|p\|$)

$$\frac{\partial \mathbf{u}}{\partial t} + \mathbf{u} \cdot \nabla \mathbf{u} + \frac{1}{\gamma M_R^2} \nabla p = 0, \quad (12)$$

$$\frac{\partial p}{\partial t} + \mathbf{u} \cdot \nabla p + \gamma \nabla \cdot \mathbf{u} = 0.$$

At $t = 0$ the initial data is

$$\mathbf{u}(\mathbf{x}, 0) = \mathbf{u}_0(\mathbf{x}), \quad (13)$$

$$p(\mathbf{x}, 0) = p_0(\mathbf{x}).$$

It is convenient for the purpose of analysis to split the velocity vector according to

$$\mathbf{u} = \mathbf{u}^I + \mathbf{u}^C, \quad (14)$$

where the solenoidal component $\mathbf{u}^I(\mathbf{x}, t)$ satisfies the time-dependent incompressible Navier-Stokes equations

$$\frac{\partial \mathbf{u}^I}{\partial t} + \mathbf{u}^I \cdot \nabla \mathbf{u}^I = -\nabla p^I, \quad (15)$$

$$\nabla \cdot \mathbf{u}^I = 0,$$

with initial conditions

$$\mathbf{u}^I(\mathbf{x}, 0) = \mathbf{u}_0^I(\mathbf{x}), \quad (16)$$

$$\nabla \cdot \mathbf{u}_0^I = 0.$$

The incompressible pressure p^I satisfies the Poisson equation

$$\nabla^2 p^I = -\nabla \mathbf{u}^I : \nabla \mathbf{u}^I \quad (17)$$

from which it is inferred that

$$p^I = O(\mathbf{u}^{I2}). \quad (18)$$

The initial solenoidal velocity is determined from the decomposition

$$\mathbf{u}_0(\mathbf{x}) = \mathbf{u}_0^I(\mathbf{x}) + \mathbf{u}_0^C(\mathbf{x}). \quad (19)$$

If the flow is homogeneous, it is easy to show that $\mathbf{u}_0^I(\mathbf{x})$ and $\mathbf{u}_0^C(\mathbf{x})$ are unique once $\mathbf{u}_0(\mathbf{x})$ is specified. When the flow is non-homogeneous, an arbitrary potential function can be added to the decomposition (19). The transverse velocity component, \mathbf{u}^I is divergence-free for all time (since it satisfies the time-dependent incompressible Navier-Stokes equations). Although \mathbf{u}^C is initially vorticity-free, it acquires a small degree of vorticity subsequently. Kreiss, Lorenz and Naughton (1990) have estimated this vorticity to be $O(M_R^2)$.

Substitution of Eq. (14) into Eqs. (12) and manipulation of the resulting expressions using Eqs. (15) yield

$$\frac{\partial \mathbf{u}^C}{\partial t} + \mathbf{u}^I \cdot \nabla \mathbf{u}^C + \mathbf{u}^C \cdot \nabla \mathbf{u}^I + \mathbf{u}^C \cdot \nabla \mathbf{u}^C = -\frac{1}{\gamma M_R^2} (\nabla p - \gamma M_R^2 \nabla p^I), \quad (20)$$

$$\frac{\partial p}{\partial t} + \mathbf{u}^I \cdot \nabla p + \mathbf{u}^C \cdot \nabla p + \gamma \nabla \cdot \mathbf{u}^C = 0.$$

The momentum equation in Eqs. (20) is simplified if the perturbation pressure is decomposed according to

$$p = \gamma M_R^2 p^I + \delta p^C. \quad (21)$$

This particular decomposition removes p^I from the evolution equation for \mathbf{u}^C . At $t = 0$,

$$p^I(\mathbf{x}, 0) = p_0^I(\mathbf{x}) \quad (22)$$

is uniquely determined from the incompressible evolution equations, so that there is no ambiguity in the computation of $p^C(\mathbf{x}, 0)$. The uniqueness of the pressure decomposition is maintained for all time. The parameter δ is defined to insure that

$$\|p^C(\mathbf{x}, 0)\| = 1. \quad (23)$$

The total initial velocity \mathbf{u} is also normalized to unity, i.e. $\|\mathbf{u}_0(\mathbf{x})\| = 1$. This is most easily accomplished by choosing

$$U_R = \|\mathbf{u}_0^*(\mathbf{x})\|. \quad (24)$$

Therefore, both \mathbf{u}_0^C and \mathbf{u}_0^I are $O(1)$. From Eq. (18), $\|p_0^I\| = O(1)$. Incompressible variables vary on a slower time scale than the acoustic time scale, which is the time scale of interest, so that their order of magnitude will remain invariant in time. In contrast, we will demonstrate that certain combinations of initial conditions can lead to time boundary layers which can change the order of magnitudes of compressible variables on a time scale of $O(M_R)$.

Substitution of Eqs. (14), (21) into the system (12) leads to the evolution equations

$$\begin{aligned}\frac{\partial \mathbf{u}^C}{\partial t} + \mathbf{u}^I \cdot \nabla \mathbf{u}^C + \mathbf{u}^C \cdot \nabla \mathbf{u}^C + A\mathbf{u}^C + \frac{\delta}{\gamma M_R^2} \nabla p^C &= 0, \\ \frac{\partial p^C}{\partial t} + \mathbf{u}^I \cdot \nabla p^C + \mathbf{u}^C \cdot \nabla p^C + B\mathbf{u}^C + \frac{\gamma}{\delta} \nabla \cdot \mathbf{u}^C &= G,\end{aligned}$$

for the compressible components of the flow variables, where

$$\begin{aligned}A\mathbf{u}^C &= \mathbf{u}^C \cdot \nabla \mathbf{u}^I, \\ B\mathbf{u}^C &= \frac{\gamma M_R^2}{\delta} \mathbf{u}^C \cdot \nabla p^I, \\ G &= -\frac{\gamma M_R^2}{\delta} \left[\frac{\partial p^I}{\partial t} + \mathbf{u}^I \cdot \nabla p^I \right].\end{aligned}$$

For reference, the orders of magnitude for A , B and G at $t = 0$ are

$$\begin{aligned}A &= O(1), \\ B &= O\left(\frac{\gamma M_R^2}{\delta}\right), \\ G &= O\left(\frac{\gamma M_R^2}{\delta}\right).\end{aligned}$$

Since A , B , G only depend on incompressible quantities, their order of magnitude is constant over the time scale of interest. The initial data is

$$\begin{aligned}\mathbf{u}^C(\mathbf{x}, 0) &= \mathbf{u}_0(\mathbf{x}) - \mathbf{u}_0^I(\mathbf{x}) = \mathbf{u}_0^C(\mathbf{x}), \\ p^C(\mathbf{x}, 0) &= p_0(\mathbf{x}) - \frac{\gamma M_R^2}{\delta} p_0^I = p_0^C(\mathbf{x}).\end{aligned}$$

Note that \mathbf{u}_0^C is vorticity-free. The pressure $P(\mathbf{x})$ is now given by

$$P(\mathbf{x}, t) = 1 + \gamma M_R^2 p^I(\mathbf{x}, t) + \delta p^C(\mathbf{x}, t). \quad (25)$$

It must be noted that although p^C and \mathbf{u}^C are $O(1)$ at $t = 0$, there is no guaranty that they will remain so. Should they exceed that order, they will be scaled down, otherwise terms might be neglected in the governing equations which should be kept.

C. Regime Classification

Freezing coefficients in Eqs. (25) makes it clear that there are two different time scales present, i.e. the convection scale of order $O(1)$, and the sound wave scale of order $O(M_R)$. Since the initial compressible velocity field $\mathbf{u}_0^C(\mathbf{x})$ is vorticity-free, we expect \mathbf{u}^C to vary on the fast acoustic time scale. Therefore we introduce a new time variable

$$t' = \frac{t}{M_R}. \quad (26)$$

In terms of t' , Eqs. (25) become

$$\frac{\partial \mathbf{u}^C}{\partial t'} + M_R [(\mathbf{u}^I + \mathbf{u}^C) \cdot \nabla \mathbf{u}^C + A \mathbf{u}^C] + \frac{\delta}{M_R \gamma} \nabla p^C = 0, \quad (27)$$

$$\frac{\partial p^C}{\partial t'} + M_R [(\mathbf{u}^I + \mathbf{u}^C) \cdot \nabla p^C + B \mathbf{u}^C] + \frac{M_R \gamma}{\delta} \nabla \cdot \mathbf{u}^C = M_R G.$$

The system of equations (27) is hyperbolic and for $\delta \ll M_R$ or $\delta \gg M_R$ it is highly asymmetric. Therefore the solution will in general grow rapidly, thus invalidating the original scalings (see appendix). Only with the symmetrized version of Eqs. (27) can we be sure that the solution at $t > 0$ is bounded by the order of magnitude of the solution at $t = 0$. Therefore we symmetrize the system in such a way that the initial data are not "scaled up" because otherwise nonlinear terms which are initially negligible may not remain so. The change of variables which leads to symmetry is dependent on whether the coefficient of ∇p^C in Eq. (27) is less or greater than unity. In terms of δ , we therefore distinguish two cases.

$$\underline{\delta \leq M_R \gamma}$$

This regime is characterized by low levels of initial acoustic pressure fluctuation. We first introduce a new dependent variable

$$p^{C'} = \frac{\delta}{M_R \gamma} p^C \quad (28)$$

which insures that

$$\|p_0^{C'}\| \leq \|p_0^C\| = O(1). \quad (29)$$

Eqs. (27) become

$$\frac{\partial \mathbf{u}^C}{\partial t'} + M_R [(\mathbf{u}^I + \mathbf{u}^C) \cdot \nabla \mathbf{u}^C + A \mathbf{u}^C] + \nabla p^{C'} = 0, \quad (30)$$

$$\frac{\partial p^{C'}}{\partial t'} + M_R [(\mathbf{u}^I + \mathbf{u}^C) \cdot \nabla p^{C'} + \frac{\delta}{\gamma M_R} B \mathbf{u}^C] + \nabla \cdot \mathbf{u}^C = \frac{\delta}{\gamma} G,$$

with initial data

$$\begin{aligned} \mathbf{u}^C(\mathbf{x}, 0) &= \mathbf{u}_0^C(\mathbf{x}), \\ p^{C'}(\mathbf{x}, 0) &= \frac{\delta}{\gamma M_R} p_0^C(\mathbf{x}). \end{aligned}$$

By construction, $\mathbf{u}^C(\mathbf{x}, 0)$ and $p^{C'}(\mathbf{x}, 0)$ are $O(1)$. If they should be much less than unity, the dependent variables are rescaled so that they become $\tilde{O}(1)$, in which case the coefficients of Eqs. (30) are replaced by smaller coefficients, and the approximations below become more valid. (The notation $f = \tilde{O}(M)$ is equivalent to

$\lim_{M \rightarrow 0} f(M)/M \neq 0 < \infty$. On the other hand, the $O(M)$ symbol only states that the limit is finite, possibly zero.) The system (30) is a well-behaved system of differential equations. However, one must check whether the convective terms remain negligible when $t' = O(1)$. It is easily shown that on the fast time scale, the lowest order evolution equations are given by the linear wave equations

$$\frac{\partial \mathbf{u}^C}{\partial t'} + \nabla p^{C'} = 0,$$

$$\frac{\partial p^{C'}}{\partial t'} + \nabla \cdot \mathbf{u}^C = 0,$$

with the initial data

$$\begin{aligned} \mathbf{u}^C(\mathbf{x}, 0) &= \mathbf{u}_0^C(\mathbf{x}), \\ p^{C'}(\mathbf{x}, 0) &= \frac{\delta}{\gamma M_R} p_0^C(\mathbf{x}). \end{aligned}$$

On the convective time scale, Kreiss et al. (1990) have shown that the wave equation still describes the acoustic component of the flow.

From the wave equation, it is now easy to predict the order of magnitude of \mathbf{u}^C and p^C as a function of initial magnitudes. After a time $t' = \tilde{O}(1)$, both \mathbf{u}^C and $p^{C'}$ will have the same order of magnitude, given by

$$\begin{aligned} \mathbf{u}^C(\mathbf{x}, t') \approx p^{C'}(\mathbf{x}, t') &= O(\max(\mathbf{u}_0^C(\mathbf{x}), p_0^{C'}(\mathbf{x}))), \\ &= O(\max(\mathbf{u}_0^C(\mathbf{x}), \frac{\delta}{\gamma M_R})). \end{aligned}$$

The results are summarized in table 1 for all different initial estimates of velocity.

\mathbf{u}_0^C	$p_0^{C'}$	\mathbf{u}_∞^C	p_∞^C
$O(1)$	$O(1)$	$O(1)$	$O(\frac{M_R \gamma}{\delta})$
$\tilde{O}(M_R^j)$	$O(1)$	$O(\max(M_R^j, \frac{\delta}{\gamma M_R}))$	$O(\max(\frac{\gamma M_R^{j+1}}{\delta}, 1))$

Table 1: Order of magnitude of equilibrium levels of compressible pressure and acoustic velocity as a function of initial levels.

With the chosen initial normalization for the velocity, \mathbf{u}^I must be $\tilde{O}(1)$, unless $\mathbf{u}^C = \tilde{O}(1)$. The choice of the initial magnitude of the incompressible velocity component partly determines the initial variation of the ratio of compressible kinetic energy to total kinetic energy.

$$\underline{\delta > M_R \gamma}$$

Now we introduce the new variable

$$\mathbf{u}^{C'} = \frac{M_R \gamma}{\delta} \mathbf{u}^C \quad (31)$$

which insures that

$$\|\mathbf{u}_0^{C'}\| \leq \|\mathbf{u}_0^C\| = O(1). \quad (32)$$

Using Eq. (31), Eqs. (27) become

$$\frac{\partial \mathbf{u}^{C'}}{\partial t'} + (M_R \mathbf{u}^I + \frac{\delta}{\gamma} \mathbf{u}^{C'}) \cdot \nabla \mathbf{u}^{C'} + M_R A \mathbf{u}^{C'} + \nabla p^C = 0, \quad (33)$$

$$\frac{\partial p^C}{\partial t'} + (M_R \mathbf{u}^I + \frac{\delta}{\gamma} \mathbf{u}^{C'}) \cdot \nabla p^C + \frac{\delta}{\gamma} B \mathbf{u}^{C'} + \nabla \cdot \mathbf{u}^{C'} = M_R G$$

with the initial data

$$\mathbf{u}^{C'}(\mathbf{x}, 0) = \frac{M_R \gamma}{\delta} \mathbf{u}_0^C(\mathbf{x}), \quad (34)$$

$$p^C(\mathbf{x}, 0) = p_0^C(\mathbf{x}) = \tilde{O}(1).$$

Once again, if the initial data in Eq. (34) should be much less than unity, a rescaling of velocity and pressure would simply decrease the coefficients of the quadratic terms. As long as $\mathbf{u}^{C'}(\mathbf{x}, t') = O(1)$, Eqs. (33) reduce to

$$\frac{\partial \mathbf{u}^{C'}}{\partial t'} + \frac{\delta}{\gamma} \mathbf{u}^{C'} \cdot \nabla \mathbf{u}^{C'} + \nabla p^C = 0, \quad (35)$$

$$\frac{\partial p^C}{\partial t'} + \frac{\delta}{\gamma} \mathbf{u}^{C'} \cdot \nabla p^C + \frac{\delta}{\gamma} B \mathbf{u}^{C'} + \nabla \cdot \mathbf{u}^{C'} = 0,$$

with initial conditions given by Eq. (34). When $t' = O(1)$,

$$\begin{aligned} \|\mathbf{u}^{C'}(\mathbf{x}, t')\| &= \|p^C(\mathbf{x}, t')\|, \\ &= \tilde{O}(\max(p_0^C, \mathbf{u}_0^{C'})), \\ &= \tilde{O}(1). \end{aligned} \quad (36)$$

Equations (31) and (36) imply that

$$\mathbf{u}^C(\mathbf{x}, t') = \tilde{O}\left(\frac{\delta}{M_R}\right). \quad (37)$$

When $\delta = \tilde{O}(1)$, the convective terms balance the time derivative terms, in which case wave steepening may occur on a $t' = O(1)$ time scale, and there is a propensity for shocks to form. Note that when shocks do occur, the turbulent Mach number, M_t is no longer small, but has increased by a factor $1/M_R$ from its initial value.

D. Results

In the previous section, we established the conditions for two separate asymptotic regimes, depending on whether the ratio of δ to γM_R was lesser or greater than unity. We now wish to deduce some physical consequences from the results of the previous section. To this end, we consider various levels of initial rms values for \mathbf{u}^C_0 and δ . The rms of \mathbf{u}^I is fixed at unity. Only when $\|\mathbf{u}^C_0\| = \tilde{O}(1)$ can $\|\mathbf{u}^I\| < \tilde{O}(1)$. It is then easily shown that the rms level of \mathbf{u}^I can be increased to unity without affecting the order of magnitude estimates at $t' = 1$.

Table 2 summarizes the theoretical findings from the previous section. To properly interpret the table, replace a cell value of, for example, 3 by $\tilde{O}(M_R^3)$. A subscript (∞) refers to the value of a variable after the initial transients have died away ($t' = \tilde{O}(1)$), also referred to as an equilibrium state. When viscous effects are taken into account, the equilibrium state of all quantities varies over the viscous time scale. They also fluctuate in time due to higher order convective effects that have been neglected to lowest order in the current expansion. For example, on the incompressible convective time scale, the terms $M_R \mathbf{u}^I \cdot \nabla \mathbf{u}^C$ induce small fluctuations of the variables about the equilibrium state of the system.

The rms levels of \mathbf{u}^C_0 and δ are given in the first two columns of table 2. The fifth and sixth columns contain the new quantity

$$\chi = \frac{\|\mathbf{u}^C\|^2}{\|\mathbf{u}^C\|^2 + \|\mathbf{u}^I\|^2} \quad (38)$$

which is the fraction of the total kinetic energy solely due to acoustic effects. Note that at $t = 0$, the denominator is unity by construction, so that

$$\|\mathbf{u}^I_0\| = \sqrt{1 - \chi_0}, \quad (39)$$

and

$$\|\mathbf{u}^C_0\| = \sqrt{\chi_0}. \quad (40)$$

From Eq. (37),

$$\chi_\infty = \frac{1}{1 + M_R^2 \|\mathbf{u}^I\|^2}, \quad (41)$$

and since $\|\mathbf{u}^I\| = O(1)$, $\delta = \tilde{O}(1)$ always implies that $\chi_\infty = \tilde{O}(1)$. Consequently, the lower the initial level of compressibility at a fixed M_R (i.e. the lower χ_0), the stronger the initial transient (which extends over the time period $O(M_R)$). As this imbalance intensifies, the propensity for shocks to form also increases. Table 2 reflects these statements in the rows corresponding to $\delta = \tilde{O}(1)$. When $\mathbf{u}^C_0 = \tilde{O}(1)$, $\mathbf{u}^I_0 = \tilde{O}(M_R^n)$, $n \geq 1$. However, the value of n does not change the previous conclusions. Based on the results in Sarkar, Erlebacher, Hussaini and Kreiss (1989), it is

straightforward to show that

$$\chi_{\infty}^{th} = \frac{1}{2} \frac{1 + \xi^2}{1 - 0.5\chi_0(1 - \xi^2)}, \quad (42)$$

where

$$\xi = \frac{\|p^c\|}{M_t \gamma}. \quad (43)$$

u^c_0	δ	u^c_{∞}	p^c_{∞}	χ_0	χ_{∞}	F_0
0	0	-1	0	0	0	2
0	1	0	0	0	0	0
0	2	0	-1	0	0	-2
0	3	0	-2	0	0	-4
1	0	-1	0	2	0	4
1	1	0	0	2	0	2
1	2	1	0	2	2	0
1	3	1	-1	2	2	-2
1	4	1	-2	2	2	-4
2	0	-1	0	4	0	6
2	1	0	0	4	0	4
2	2	1	0	4	2	2
2	3	2	0	4	4	0
2	4	2	-1	4	4	-2
2	5	2	-2	4	4	-4

Table 2: Estimates of equilibrium levels of compressible pressure (p^c), (u^c), χ as a function of a wide range of initial levels for p^c and u^c . Table entries should be interpreted as $\tilde{O}(M_R^{\text{table entry}})$.

Two separate regimes (different from the mathematical regimes of the previous section) are apparent from table 2. For large values of δ , $\|p^c_{\infty}\| = \tilde{O}(1)$, while u^c increases sharply. This sudden increase over the acoustic time scale is most important when δ is large and u^c_0 is small. The fact that this increase in the acoustic velocity is not contingent on $\delta = \tilde{O}(1)$ indicates that an initial imbalance in compressible energy can occur without the need to appeal to wave steepening. When δ is sufficiently small, u^c remains at its initial level and large pressure waves appear in the flow. The compressible pressure imbalance becomes more severe with decreasing u^c_0 and decreasing δ . Equilibrium initial conditions are characterized by the juncture between the two aforementioned regimes. This corresponds to

$$u^c_0 = \tilde{O}\left(\frac{\delta}{M_R}\right). \quad (44)$$

Using Eq. (39), Eq. (44) becomes

$$\frac{M_R^2 \chi_0}{\delta^2} = \bar{O}(1). \quad (45)$$

The function

$$F(t) = \frac{\gamma^2 M_R^2 \chi}{\delta^2} \quad (46)$$

was introduced by Sarkar et al. (1989) and shown to play a fundamental role in the description of compressible turbulence. The last column in table 2 tabulates the value of $F_0 = F(0)$ for the various cases. It is now easy to see that a necessary condition for the appearance of shocks is $\delta = 1$ (see previous section). If the latter condition is not satisfied, the level of compressibility will remain small for all time, which is inconsistent with the appearance of an isotropic distribution of shocks.

It is interesting to establish the conditions under which p^C is a good approximation to the total perturbation pressure p . To this end consider the relation between p^C , p^I and p :

$$\delta^2 \|p^C\|^2 = \|p\|^2 + \gamma^2 M_R^4 \|p^I\|^2 \quad (47)$$

which is justified if $p(\mathbf{x})$ and $p^I(\mathbf{x})$ are assumed to be decorrelated. This is true by construction at $t = 0$ in our direct numerical simulation code (discussed in a later section). From Eq. (18), $\|p^I\|$ and $\|u^I\|$ are related by

$$\begin{aligned} \|p^I\| &= \alpha_1 \|u^I\|^2, \\ &= \alpha_1 (1 - \chi_0), \end{aligned} \quad (48)$$

where α_1 is an assumed $\bar{O}(1)$ constant. Using Eq. (48), Eq. (47) becomes

$$\delta^2 \|p^C\|^2 = \|p_0\|^2 + \gamma^2 M_R^4 \alpha_1^2 (1 - \chi_0)^2. \quad (49)$$

The incompressible component of the pressure field is therefore negligible when

$$\|p_0\| \gg \gamma M_R^2 \alpha_1 (1 - \chi_0). \quad (50)$$

This result will be verified with the help of direct numerical simulations. Equation (50) tells us that one cannot neglect the influence of p^I at higher levels of M_R and at lower levels of the initial compressibility ratio, χ_0 .

III. Numerical Simulation

A. Numerical Algorithm

Our direct simulations of two-dimensional compressible turbulence are based on Eqs. (1). The flow is assumed to be isotropic. Hence a double Fourier representation is appropriate. Spectral methods, by nature of their high accuracy and low dispersive and dissipative errors are ideally suited for this problem. Spatial derivatives are approximated

by Fourier collocation (Canuto, Hussaini, Quarteroni and Zang 1988). In each coordinate direction, N grid points are used; for example $x_j = 2\pi j/N$, $j = 0, 1, \dots, N-1$ in the x direction. The derivative of a function $\mathcal{F}(\mathbf{x})$ with respect to x is calculated from the analytic derivative of the trigonometric interpolant of $\mathcal{F}(\mathbf{x})$ in the direction x . Many simulations of incompressible, homogeneous turbulence have used a Fourier-Galerkin method. The compressible equations, however, contain cubic rather than quadratic nonlinearities and true Galerkin methods are more expensive (compared with collocation methods) than they are for incompressible flow. The essential difference between collocation and Galerkin methods is that the former are subject to both truncation and aliasing errors, whereas the latter have only truncation errors. As discussed extensively by Canuto, et al. (1988), the aliasing terms are not significant for a well-resolved flow. However, care is needed to pose the relevant equations for a collocation method in a form which ensures numerical stability. For this reason, the convective term in the momentum equations is actually used in the equivalent form

$$\frac{1}{2}[\nabla \cdot (\rho \mathbf{u} \mathbf{u}) + \rho \mathbf{u} \cdot \nabla \mathbf{u} + \mathbf{u} \nabla \cdot (\rho \mathbf{u})]. \quad (51)$$

As noted by Feiereisen, Reynolds and Ferziger (1981), this form, together with a symmetric differencing method in space (for example Fourier collocation), ensure conservation of mass and momentum. Moreover, energy is conserved for the semi-discrete inviscid equations.

We are interested in the low subsonic regime $M_R \ll 1$. The sound speed is in this case much greater than the flow velocity and this imposes a severe restriction on the time step of any explicit time marching numerical scheme. To remove this constraint, a splitting method is adopted. The first step integrates implicitly

$$\begin{aligned} \frac{\partial \rho}{\partial t} &= 0, \\ \frac{\partial(\rho \mathbf{u})}{\partial t} + \frac{1}{2}[\nabla \cdot (\rho \mathbf{u} \mathbf{u}) + \mathbf{u} \cdot \nabla(\rho \mathbf{u}) + \rho \mathbf{u} \cdot \nabla \mathbf{u}] &= \frac{1}{Re} \nabla \cdot \vec{\sigma}, \\ \frac{\partial P}{\partial t} + \mathbf{u} \cdot \nabla P + \gamma P \nabla \cdot \mathbf{u} - c_0^2 \nabla \cdot (\rho \mathbf{u}) &= \\ \frac{\gamma}{Re Pr} \nabla^2 T + \frac{\gamma(\gamma-1)M_R^2}{Re} \Phi, \end{aligned} \quad (52)$$

from which the acoustic effects that vary on the fast time scale $O(M_R)$ have been removed. The second step integrates the "acoustic equations" which vary on the fast time scale. These equations are

$$\begin{aligned} \frac{\partial \rho}{\partial t} + \nabla \cdot (\rho \mathbf{u}) &= 0, \\ \frac{\partial \rho \mathbf{u}}{\partial t} + \frac{1}{\gamma M_R^2} \nabla P &= 0, \\ \frac{\partial P}{\partial t} + c_0^2 \nabla \cdot (\rho \mathbf{u}) &= 0. \end{aligned} \quad (53)$$

where c_0 is the root mean square (rms) of the sound speed.

This splitting is employed at each stage of a low-storage third-order Runge-Kutta method. To minimize the errors due to the large implicit time step, Eqs. (53) are integrated analytically. In Fourier space the system (53) become

$$\begin{aligned}\frac{\partial \hat{\rho}}{\partial t} + \iota \mathbf{k} \cdot \hat{\mathbf{m}} &= 0, \\ \frac{\partial \hat{\mathbf{m}}}{\partial t} + \frac{\iota \mathbf{k}}{\gamma M_R^2} \hat{P} &= 0, \\ \frac{\partial \hat{P}}{\partial t} + \iota c_0^2 \mathbf{k} \cdot \hat{\mathbf{m}} &= 0,\end{aligned}\quad (54)$$

where $\hat{\mathbf{m}} = \rho \hat{\mathbf{u}}$ and Fourier transformed quantities, which depend upon the wavenumber \mathbf{k} , are denoted by a circumflex. Equations (54) are solved exactly in Erlebacher, Hussaini, Speziale and Zang (1987) and are rewritten here for completeness:

$$\begin{aligned}\hat{\rho}^{(2)} &= \hat{\rho}^{(1)} + \frac{1}{c_0^2} [\hat{A} \cos(\frac{c_0 k \Delta t_s}{M_R \sqrt{\gamma}}) + \hat{B} \sin(\frac{c_0 k \Delta t_s}{M_R \sqrt{\gamma}}) - \hat{A}], \\ \hat{\mathbf{m}}^{(2)} &= \hat{\mathbf{m}}^{(1)} - \frac{i \mathbf{k}}{c_0 k M_R \sqrt{\gamma}} [\hat{A} \sin(\frac{c_0 k \Delta t_s}{M_R \sqrt{\gamma}}) - \hat{B} \cos(\frac{c_0 k \Delta t_s}{M_R \sqrt{\gamma}}) + \hat{B}], \\ \hat{P}^{(2)} &= \hat{A} \cos(\frac{c_0 k \Delta t_s}{M_R \sqrt{\gamma}}) + \hat{B} \sin(\frac{c_0 k \Delta t_s}{M_R \sqrt{\gamma}}),\end{aligned}\quad (55)$$

where $k = |\mathbf{k}|$ is the magnitude of the Fourier wavevector, $\hat{A} = \hat{P}^{(1)}$, $\hat{B} = i \frac{c_0}{k} \mathbf{k} \cdot \hat{\mathbf{m}}^{(1)}$. Superscripts 1 and 2 relate to the end of the first and second fractional step respectively. The effective time-step of the Runge-Kutta stage is denoted by Δt_s . The advantage of this splitting is that the principal terms responsible for the acoustic waves have been isolated. Since they are treated semi-implicitly, one expects the explicit time-step limitation to depend upon $v + |c - c_0|$ rather than $v + c$. (Although there is also a viscous stability limit for the first fractional step, it is well below the advection limit in the cases of interest.) This is clearly efficient at low Mach numbers. Since the second fractional step is integrated analytically, it does not generate dispersion or dissipation errors. The only errors incurred are time splitting errors.

If one is truly interested in the detailed time-evolution of the acoustic components, the time-step must be small enough to resolve the temporal evolution of these waves. Note however, that because the acoustics are treated exactly in the second step, the large time step simulation still produces accurate results, but the data is not available at intermediate times.

The expected stability limit of this two-dimensional Fourier collocation method for the compressible Navier-Stokes equations has the form

$$\Delta t < \alpha \min\left(\frac{\Delta x}{|u| + |c - c_0|} + \frac{\Delta y}{|v| + |c - c_0|}\right).\quad (56)$$

For the third-order Runge-Kutta method employed here $\alpha = 0.54$. For accuracy purposes, the results herein are all based on $\alpha = 0.1$.

B. Initial Conditions

The initial conditions for the direct numerical simulations presented here are similar to those presented by Passot and Pouquet (1987). They are sufficiently general to produce the various turbulent regimes we expect to occur when $M_R \ll 1$. One must separately specify the reference Mach number M_R , the Reynolds number, Re , the Prandtl number, Pr , the rms levels of \mathbf{u}_0^C , \mathbf{u}_0^I , $\|\rho_0\|$, $\|T_0\|$, and the autocorrelation spectrum for ρ , T , \mathbf{u}^C and \mathbf{u}^I . We now detail the procedure used in the numerical code.

We first generate random fields in physical space in the range $[-0.5, 0.5]$ for \mathbf{u}_0 , ρ_0 , and T_0 . Next, the velocity is decomposed into the sum

$$\mathbf{u}_0(\mathbf{x}) = \mathbf{u}_0^C(\mathbf{x}) + \mathbf{u}_0^I(\mathbf{x}) \quad (57)$$

where

$$\begin{aligned} \nabla \cdot \mathbf{u}_0^I &= 0, \\ \nabla \times \mathbf{u}_0^C &= 0. \end{aligned}$$

This decomposition is unique for homogeneous flows and is accomplished in Fourier space according to the prescription

$$\begin{aligned} \hat{\mathbf{u}}^I &= \hat{\mathbf{u}} - \frac{\mathbf{k} \cdot \hat{\mathbf{u}}}{k^2} \mathbf{k}, \\ \hat{\mathbf{u}}^C &= \hat{\mathbf{u}} - \hat{\mathbf{u}}^I. \end{aligned}$$

After transforming the velocity components back to physical space, we rescale \mathbf{u}^C , \mathbf{u}^I , ρ , and T to impose a prescribed autocorrelation spectrum. The autocorrelation spectrum $E_{pp}(\mathbf{k})$ of a variable $p(\mathbf{x})$ is defined as

$$\int p(\mathbf{x})p(\mathbf{x})d\mathbf{x} = \int E_{pp}(k)dk. \quad (58)$$

For example, the 2D energy spectrum for \mathbf{u} , i.e. $E(k)$, is the autocorrelation spectrum $E_{\mathbf{u} \cdot \mathbf{u}}$.

We now impose the spectrum

$$E(k) = k^4 e^{-\frac{k^2}{2k_0^2}} \quad (59)$$

on each of the variables. The procedure for imposing the required spectrum $E(k)$ is explained using the density as an example. One scans the wavenumber space, and

for each pair (k_x, k_y) , the corresponding spherical shell is determined. The i^{th} shell is defined by

$$(i - \frac{1}{2} < k < i + \frac{1}{2}). \quad (60)$$

where $k = \sqrt{k_x^2 + k_y^2}$. All spherical shells have unit width. The 0^{th} shell is empty because $\mathbf{k} = (0, 0)$ is the mean component which does not contribute to the autocorrelation spectrum. The contribution of the i^{th} shell to the autocorrelation spectrum thus becomes

$$E_i^* = \sum_{i-\frac{1}{2} < k < i+\frac{1}{2}} |\hat{\rho}(\mathbf{k})|^2 \quad (61)$$

where E_i^* is the discrete representation of $\int_{i-\frac{1}{2}}^{i+\frac{1}{2}} E^*(k) dk$. (For 2-D flows, spherical should be interpreted as circular.) Defining E_i as

$$E_i = E(i) \quad (62)$$

where $E(i)$ is obtained from Eq. (59), the density is rescaled according to

$$\hat{\rho}(i) \leftarrow \hat{\rho}(i) \sqrt{\frac{E_i}{E_i^*}} \quad (63)$$

in order to impose the desired spectrum. In a similar way, the autocorrelation spectra for \mathbf{u}^c , \mathbf{u}^f and T are calculated. For the velocity, the procedure is identical to that described for ρ , except that the scalar ρ is replaced by a vector, and $|\hat{\rho}(\mathbf{k})|^2$ is replaced by $|\hat{\mathbf{u}}(\mathbf{k})|^2$.

It is still possible to rescale these quantities by an arbitrary constant in physical space without changing the properties of its autocorrelation spectrum. Therefore, we impose given rms levels for ρ , T and \mathbf{u} by an appropriate rescaling. There still remains a degree of freedom on the velocity, since \mathbf{u}^c and \mathbf{u}^f can be weighted independently without affecting the rms of \mathbf{u} . Therefore, we specify the initial level of compressibility in the flow according to

$$\chi = \frac{\int \mathbf{u}^c \cdot \mathbf{u}^c dx}{\int (\mathbf{u}^c \cdot \mathbf{u}^c + \mathbf{u}^f \cdot \mathbf{u}^f) dx}. \quad (64)$$

The denominator of Eq. (64) is the total kinetic energy of the system since $\int \mathbf{u}^c \cdot \mathbf{u}^f = 0$ by construction.

The mean values of ρ and T are then added to the thermodynamic variables to obtain

$$\begin{aligned} \rho &\leftarrow 1 + \rho, \\ T &\leftarrow 1 + T. \end{aligned}$$

The reference pressure in the code is chosen to be $P_R = \rho_R U_R^2$; consequently the nondimensional pressure is then calculated from

$$p = \frac{\rho T}{\gamma M_R^2} \quad (65)$$

where ρ and T are respectively the non-dimensional density and temperature. The turbulent Mach number M_t is related to the reference Mach number M_R according to Eq. (6).

IV. Numerical Validation of Theory

In this section, we show results of 2-D direct numerical simulations on grids of 64×64 to validate the theory described in the preceding sections. This validation is accomplished by comparing the value of χ after several acoustic periods as predicted by the computation, against that given by the theory. The parameter F , defined by Eq. (46) is also computed and compared with numerical results.

Given the large parameter space, in every run, the density and temperature fluctuation rms levels are set equal to each other. An extensive parameter range is covered by considering all combinations of

$$\begin{aligned}\chi_0 &= (0.1, 0.5, 0.9), \\ M_R &= (0.03, 0.08, 0.3), \\ \|\rho\| = \|T\| &= (0.01, 0.05, 0.1).\end{aligned}$$

Cases are referred to by a 3 digit combination. For example, case 123 refers to $\chi_0 = 0.1$, $M_R = 0.08$ and $\|\rho\| = \|T\| = 0.10$. Simulations are run at $Re = 150$, $\|u\| = 1$, $k_0 = 10$. This corresponds to a microscale Reynolds number $R_\lambda = 20$. The various diagnostics are computed at every iteration.

The quantities considered for comparison between the numerical computations and the theory results are

$$F = \left(\frac{\gamma M_R}{p^c} \right)^2 \left\| \frac{u^2}{T} \right\| \chi \quad (66)$$

and χ . Both these quantities are computed by averaging them over several consecutive iterations: χ is averaged over iterations 5 to 10 (χ_{5-10}) and 10 to 15 (χ_{10-15}), while F is averaged over iterations 10-15 (F_{10-15}). Their equilibrium values χ_∞ and F_∞ are computed by averaging their values over the last 60 iterations of the 400 iteration numerical simulation. The two sets of averages for χ give an idea of the convergence rate of χ towards the theoretical prediction χ^{th} . If χ is averaged over too few time steps, the value could be either over or under predicted since $\chi(t)$ is an oscillatory integral which tends to unity. On the other hand, if χ is averaged over too many steps, the effects of viscosity will be noticeable, and agreement with χ_∞^{th} will not be reached. Averages over five iterations prove adequate.

Table 3 summarizes the simulation results. Note that χ_{10-15} is in closer agreement with χ_∞^{th} than is χ_{5-10} . On the other hand the average χ decays as a function of

case	χ_{5-10}	χ_{10-15}	χ_{∞}	χ_{∞}^{th}	F_0	F_{10-15}	F_{∞}	$\delta/ p_0 $
111	0.11	0.11	0.08	0.11	1.00	1.01	1.01	1.00
112	0.63	0.62	0.44	0.62	0.03	0.98	1.01	1.00
113	0.90	0.86	0.76	0.87	0.01	0.98	0.99	1.00
121	0.06	0.06	0.05	0.06	6.15	1.00	1.00	1.05
122	0.25	0.21	0.14	0.22	0.25	0.92	1.00	1.00
123	0.58	0.52	0.32	0.49	0.06	1.68	0.99	1.00
131	0.08	0.05	0.06	0.05	86.5	0.73	0.93	5.10
132	0.09	0.07	0.06	0.07	3.46	0.88	0.96	1.39
133	0.11	0.13	0.09	0.11	0.87	1.09	0.95	1.10
211	0.38	0.38	0.24	0.38	4.32	1.03	1.01	1.00
212	0.77	0.77	0.59	0.77	0.17	1.01	1.00	1.00
213	0.94	0.92	0.84	0.92	0.04	0.96	0.99	1.00
221	0.30	0.35	0.21	0.34	30.7	1.07	1.01	1.01
222	0.47	0.47	0.29	0.47	1.23	0.93	0.99	1.00
223	0.73	0.69	0.29	0.68	0.31	1.23	1.00	1.00
231	0.40	0.27	0.47	0.33	432.	0.69	0.96	2.93
232	0.40	0.29	0.20	0.35	17.3	0.71	0.96	1.12
233	0.42	0.35	0.23	0.38	4.33	0.79	0.99	1.03
311	0.84	0.84	0.67	0.83	7.78	1.03	1.01	1.00
312	0.95	0.95	0.88	0.95	0.31	1.02	1.00	1.00
313	0.99	0.98	0.92	0.98	0.08	0.93	0.99	1.00
321	0.78	0.83	0.63	0.82	55.3	1.07	1.03	1.00
322	0.86	0.86	0.70	0.87	2.22	0.96	1.01	1.00
323	0.94	0.92	0.81	0.93	0.55	1.06	0.99	1.00
331	0.85	0.76	0.63	0.82	778.	0.71	1.02	1.12
332	0.85	0.77	0.63	0.82	31.2	0.72	1.01	1.00
333	0.86	0.80	0.64	0.83	7.80	0.79	1.01	1.00

Table 3: Comparison of two-dimensional direct simulation data against theoretical predictions. All symbols are defined in the text.

time in part due to viscous effects which is reflected by the low values of χ_∞ compared to χ_∞^{th} in the table.

Sarkar et al. (1989) showed analytically that, for low Mach number turbulence, the parameter F approaches, and then oscillates about a value of $F_\infty = 1$. Table 3, regarding F_∞ are in agreement with this result. The value of F depends on the compressible component of pressure, δp^C , not p . Nonetheless, it is p , not p^C which is used to compute F for table 3. Furthermore, the time interval, required to obtain a good average over the acoustic oscillations also increases with M_R . This explains why F_{10-15} is not close to unity at the higher values of M_R . The last column measures the departure of the initial compressible rms pressure from the initial rms pressure. The cases where $\delta/||p_0|| > 1$ correlate well with a non-equilibrium value of F after 15 iterations. On the viscous time scale, F is nonetheless close to unity in all cases, which reflects that the turbulent Mach number has decreased substantially (see Eq. (50)), i.e. p^I has become negligible with respect to p^C .

The ratio of χ_{10-15} to χ_∞^{th} is furthest from unity when $M_R = 0.3$, which is explained by the longer acoustic time scale. Since the averages are computed over a fixed number of iterations, the sample length at $M_R = 0.3$ is not adequate, and the prediction for χ_∞ is not very good. The lower value of χ_∞ with respect to χ_∞^{th} arises because χ decays on the viscous time-scale. On the other hand, F remains close to unity, and is basically unaffected by the viscosity terms.

Turbulent simulations with initial flowfields for which $F_0 = 1$ preclude initial time boundary-layers which might otherwise impose stringent restrictions on time-stepping and code accuracy. We now derive an implicit relation for χ as a function of M_R and $||p||$. To this end, we begin by collecting the required formulas. Henceforth, all quantities refer to initial conditions that are consistent with an equilibrium ($F = 1$). Based on a general velocity decomposition

$$\mathbf{u} = \alpha(\mathbf{u}^C + \beta\mathbf{u}^I) \quad (67)$$

where α is such that $||\mathbf{u}|| = 1$, the compressible to total kinetic energy ratio is written as

$$\chi = \frac{||\mathbf{u}^C||^2}{||\mathbf{u}^C||^2 + \beta^2||\mathbf{u}^I||^2} = \frac{||p^C||^2}{\gamma^2 M_R^2}, \quad (68)$$

and the rms of the compressible pressure field becomes

$$\begin{aligned} ||p^C||^2 &= ||p||^2 + \gamma^2 M_R^4 ||p^I||^2, \\ &= ||p||^2 + \gamma^2 M_R^4 \alpha_1^2 \beta^2 ||\mathbf{u}^I||^4, \end{aligned}$$

where we have assumed that p and p^I are decorrelated. By construction, they are decorrelated at $t = 0$ in the numerical code from Eq. (21) More realistically however, p^I and p^C are probably decorrelated since the incompressible and compressible components of the flowfield evolve quasi-independently.

From the previous set of equations one obtains

$$\|p\|^2 = \gamma^2 M_R^2 [\chi - \alpha_1^2 M_R^2 (1 - \chi)^2]. \quad (69)$$

Contour plots of χ are shown in Figure 1 ($\alpha_1 = 1$). It is seen that for moderate to high values of χ , the relationship between $\|p\|$ and M_R is linear, which simply restates that $\|p^C\|$ and $\|p\|$ are approximately equal. At low values of χ , $\|p\|$ decreases, and eventually reaches zero. In other words, in a turbulent flow in acoustic equilibrium ($F = 1$), high rms pressure at high turbulent Mach numbers imply that χ is close to unity. Since a necessary condition for the generation of shocks is $\delta = \tilde{O}(1)$, it follows that when shocks are present in a turbulent compressible homogeneous flow in acoustic equilibrium, the compressible part of the flow must dominate.

V. Conclusions

In this paper, an asymptotic theory that is based on an initial-value formulation of the equations of motion for compressible homogeneous turbulent flow has been presented. The expansion parameter is the turbulent Mach number, which is assumed to be small. A key feature of the theory is the decomposition of the turbulent velocity field into two physically meaningful components. The first is solenoidal and satisfies the time-dependent incompressible Navier-Stokes equations. This uniquely determines the second component which is initially irrotational, but acquires a small amount of vorticity at later times. One consequence of this decomposition, is the simultaneous separation of the pressure field into incompressible and compressible components. The incompressible component is proportional to M_R^2 .

To lowest order, the asymptotic theory describes the acoustic part of the flow by a wave equation which is coupled to the solenoidal flow through the initial conditions. At later times, stronger coupling will occur through the neglected convective and viscous terms in the momentum equation. Order of magnitude estimates permit an a priori estimate of the compressibility levels of the flow as a function of the initial conditions. It is found that the initial flow can evolve towards two basically different states (in the absence of shocks). If $F_0 < 1$, the pressure fluctuations remain at their initial levels, while the velocity fluctuations increase in such a way that χ becomes $\tilde{O}(1)$. On the other hand, if $F_0 > 1$, large pressure waves develop over a time of $\tilde{O}(M_R)$, and the rms level of the acoustic velocity remains constant. This transient behavior is well described by the solution to the wave equation, and has been checked against extensive two-dimensional direct numerical simulations. Note however that the theory is also valid for three-dimensional turbulent flows and spot checks have been conducted.

It has also been established that a necessary, but not sufficient, condition for the generation of shocks is that the flow must be in an initial state of disequilibrium (i.e. $F < 1$) which results from an initial pressure level which is $O(1)$.

Several issues need further clarification. First, it is still not clear if there are more stringent initial conditions which could guarantee the emergence of isotropic shock distributions in two or three-dimensional compressible turbulent flows. Moreover, it is not clear how the theory should be modified if the reference Mach number is no longer small. Second, the current paper only treated the lowest order equations which resulted from the asymptotic expansions. To understand the evolution of the turbulent flow on the convective and viscous time scales, it is necessary to keep both viscous terms, and higher order terms in the Mach number expansion. These higher order terms will allow an explicit computation of the effects of the incompressible eddies on the acoustic waves and vice versa. These two issues, are now being studied and will be the focus of future publications.

VI. Acknowledgements

The authors would like to thank T. Zang and C. Speziale for interesting discussions and comments on the paper.

REFERENCES

- Canuto, C.; Hussaini, M. Y.; Quarteroni, A.; and Zang, T. A. 1988 - *Spectral Methods in Fluid Dynamics*, Springer-Verlag, Berlin.
- Chu, B.T.; and Kovasznay, L.S.G. 1958 - Nonlinear Interactions in a Viscous Heat-Conducting Compressible Gas. *J. Fluid Mech.* **3**, 494.
- Dwoyer, D.L.; Hussaini, M.Y.; and Voigt, R.G. (Eds.) 1984 - *Theoretical Approaches to Turbulence*, Springer-Verlag, New-York.
- Erlebacher, G.; Hussaini, M.Y.; Speziale, C.G.; and Zang, T.A. 1987 - Toward the Large-Eddy Simulation of Compressible Turbulent Flows. ICASE Report No. 87-20 .
- Feiereisen, W.J.; Reynolds, W.C.; and Ferziger, J.H. 1981 - Simulation of a Compressible Homogeneous Turbulent Shear Flow. Rep. TF-13. Thesis. Stanford University.
- Kadomtsev, B.B.; and Petviashvili, V.I. 1973 - Acoustic Turbulence. *Sov. Phys. Dokl.* **18**, 115.
- Kovasznay, L.S.G. 1957 - Turbulence in Supersonic Flows. *J. Aero. Sciences* **20**, No. 10, 657-682.

- Kreiss, H.O.; Lorenz; and Naughton, M., 1990 - Convergence of the Solutions of the Compressible to the Solution of the Incompressible Navier-Stokes Equations. To appear in *Advances in Applied Mathematics*.
- Lighthill, M.J. 1952 - On Sound Generated Aerodynamically. I. General Theory. *Proc. Roy. Soc. A211*, No. 1107, 504-587.
- Lighthill, M.J. 1954 - On Sound Generated Aerodynamically. II. Turbulence as a Source of Sound, *Proc. Roy. Soc A222*, No. 1148, 10-32.
- Lighthill, M.J. 1956 - Viscosity Effects in Sound Waves of Finite-Amplitude. In *Surveys in Mechanics*, (Eds. G.K. Batchelor and R.M. Davies), Cambridge University Press, 1956, 250-350.
- Lumley, J.L. 1989 - The Return to Isotropy in a Compressible Flow. Report FDA-89-09, Sibley School of Mechanical and Aerospace Engineering, Cornell University.
- L'vov, V.S.; and Mikhailov, A.V. 1978a - Sound and Hydrodynamic Turbulence in a Compressible Liquid. *Sov. Phys. J. Exp. Theor. Phys.* **47**, 756.
- L'vov, V.S.; and Mikhailov, A.V. 1978b - Scattering and Interaction of Sound with Sound in a Turbulent Medium. *Sov. Phys. J. Exp. Theor. Phys.* **47**, 840.
- Moiseev, S.S.; Sagdeev, R.Z.; Tur, A.V.; and Yanovskii, V.V. 1977 - Structure of Acoustic-Vortical Turbulence. *Sov. Phys. Dokl.* **22**, 582.
- Monin, A.S.; and Yaglom, A.M. 1967 - *Statistical Fluid Mechanics*, **2**, MIT Press, Cambridge, Massachusetts.
- Moyal, J.E. 1952 - The Spectra of Turbulence in a Compressible Fluid; Eddy Turbulence and Random Noise. *Proc. of the Cambridge Phil. Soc.*, **48**, part 1, 329-344.
- Passot, T.; and Pouquet, A. 1987 - Numerical Simulation of Compressible Homogeneous Flows in the Turbulent Regime. *J. Fluid Mech.* **181** 441-466.
- Sarkar, S.; Erlebacher, G.; Hussaini, M.Y.; and Kreiss, H.O. 1989 - The Analysis and Modeling of Dilatational Terms in Compressible Turbulence. ICASE Report No. 89-79.
- Tanuiti, T.; and We, C.C. 1968 - Reductive Perturbation Method in Nonlinear Wave Propagation. I. *J. Phys. Soc. of Japan*, **24**, No. 4, 941-946.
- Tatsumi, T.; and Tokunaga, H. 1974 - One-Dimensional Shock-Turbulence in a Compressible Fluid. *J. Fluid Mech.* **65**, 581.
- Tokunaga, H.; and Tatsumi, T. 1975 - Interaction of Plane Nonlinear Waves in a Compressible Fluid and Two-Dimensional Shock-Turbulence. *J. Phys. Soc. Japan* **38** 1167.

Appendix A

I. Appendix

We want to explain the behavior of hyperbolic systems which are far from symmetric. Let us first consider the system of ordinary differential equations

$$\mathbf{u}_t = A\mathbf{u} = \begin{pmatrix} 0 & \iota a \\ -\iota a & 0 \end{pmatrix} \mathbf{u}, \quad \mathbf{u} = \begin{pmatrix} u_1 \\ u_2 \end{pmatrix}, \quad (\text{A1})$$

with initial data

$$\mathbf{u}(0) = \mathbf{u}_0. \quad (\text{A2})$$

The matrix A is antisymmetric ($A^T = -A$) so the eigenvalues μ_j , ($j = 1, 2$) are purely imaginary and the corresponding eigenvectors \mathbf{y}_j are orthonormal with respect to the scalar product

$$\langle \mathbf{u}, \mathbf{v} \rangle = \bar{u}_1 v_1 + \bar{u}_2 v_2, \quad |\mathbf{u}|^2 = \langle \mathbf{u}, \mathbf{u} \rangle, \quad (\text{A3})$$

where an overbar denotes complex conjugate. The general solution of Eq. (A1) is given by

$$\mathbf{u}(t) = \sigma_1 e^{\iota\mu_1 t} \mathbf{y}_1 + \sigma_2 e^{\iota\mu_2 t} \mathbf{y}_2 \quad (\text{A4})$$

where

$$\sigma_1 = \langle \mathbf{y}_1, \mathbf{u}_0 \rangle, \quad \sigma_2 = \langle \mathbf{y}_2, \mathbf{u}_0 \rangle. \quad (\text{A5})$$

From the orthogonality of the eigenvectors,

$$|\mathbf{u}(t)|^2 = |\sigma_1|^2 + |\sigma_2|^2 = |\mathbf{u}(0)|^2, \quad (\text{A6})$$

and the amplitude of the solution does not change. This is true for any antisymmetric matrix which can be shown by the energy method

$$\begin{aligned} \frac{\partial}{\partial t} |\mathbf{u}(t)|^2 &= \frac{\partial}{\partial t} \langle \mathbf{u}, \mathbf{u} \rangle \\ &= \langle \mathbf{u}_t, \mathbf{u} \rangle + \langle \mathbf{u}, \mathbf{u}_t \rangle \\ &= \langle A\mathbf{u}, \mathbf{u} \rangle + \langle \mathbf{u}, A\mathbf{u} \rangle \\ &= -\langle \mathbf{u}, A\mathbf{u} \rangle + \langle \mathbf{u}, A\mathbf{u} \rangle \\ &= 0. \end{aligned}$$

The fourth equality is a direct consequence of the pure imaginary eigenvalues of A . Now consider the system

$$\mathbf{u}_t = a \begin{pmatrix} 0 & \iota \\ \iota\epsilon^{-1} & 0 \end{pmatrix} \mathbf{u}. \quad (\text{A7})$$

Introducing the new variable

$$\tilde{\mathbf{u}} = \begin{pmatrix} 1 & 0 \\ 0 & \epsilon^{1/2} \end{pmatrix} \mathbf{u}, \quad (\text{A8})$$

we obtain the antisymmetric system

$$\tilde{\mathbf{u}}_t = \epsilon^{-1/2} a \begin{pmatrix} 0 & \iota \\ -\iota & 0 \end{pmatrix} \tilde{\mathbf{u}}. \quad (\text{A9})$$

By the previous result,

$$\begin{aligned} |\tilde{\mathbf{u}}(t)|^2 &= |\tilde{u}_1(t)|^2 + |\tilde{u}_2(t)|^2 \\ &= |\tilde{u}_1(0)|^2 + |\tilde{u}_2(0)|^2 \\ &= |u_1(0)|^2 + \epsilon |u_2(0)|^2. \end{aligned}$$

Assume now that $u_1(0) = O(1)$ and $u_2(0) = O(\epsilon^{1/2})$. The general form (A4) of the solution tells us that in general both $\tilde{u}_1(t) = O(1)$ and $\tilde{u}_2(t) = O(1)$. Therefore we obtain for the original variables

$$\begin{aligned} u_1(t) &= \tilde{u}_1(t) = O(1) \\ u_2(t) &= \epsilon^{-1/2} \tilde{u}_2(t) = O(\epsilon^{-1/2}) \end{aligned}$$

which shows that the amplitude

$$|\mathbf{u}(t)| = O(\epsilon^{-1/2}) |\mathbf{u}(0)| \quad (\text{A10})$$

increases dramatically for sufficiently small ϵ though the eigenvalues of A are still purely imaginary. We can also express the result in the following way. Assume that $u_1(0) = 0$ and $u_2(0) = 1$. Then $|\tilde{\mathbf{u}}(t)|^2 = \epsilon$ and

$$|\mathbf{u}(t)| = 1, \quad (\text{A11})$$

i.e. for this initial data, the amplitude does not increase. If we now make a small perturbation in $u_1(0)$, say $u_1(0) = \eta$, then the perturbation will be amplified such that $u_1(t) \approx O(1 + \epsilon^{-1/2}\eta)$ and $u_2(t) \approx O(1 + \epsilon^{-1/2}\eta)$. Thus if $\eta \gg \epsilon^{1/2}$ the perturbation destroys the solution.

There are no difficulties in generalizing the results. Consider the system

$$\mathbf{u}_t + A\mathbf{u} = 0, \quad (\text{A12})$$

where A is an $n \times n$ matrix and \mathbf{u} is a vector with n components. Assume that there is a diagonal transformation

$$D = \text{diag}(d_1, \dots, d_n), \quad 0 < d_j \leq 1, \quad (\text{A13})$$

such that DAD^{-1} is antisymmetric. Then the amplitude of the solution can grow by a factor $\max_j d_j^{-1}$, i.e.

$$|\mathbf{u}(t)| = O(\max_j d_j^{-1}) |\mathbf{u}(0)|. \quad (\text{A14})$$

In particular, if we initialize the data such that

$$|\mathbf{u}(t)| \approx |\mathbf{u}(0)|, \quad (\text{A15})$$

then we can find perturbations η which grow to the order $\max_j d_j^{-1} \eta$.

After Fourier transform, a hyperbolic system

$$\mathbf{u}_t = A\mathbf{u}_x \quad (\text{A16})$$

becomes

$$\hat{\mathbf{u}}_t = i\omega A\hat{\mathbf{u}}. \quad (\text{A17})$$

The eigenvalues of $i\omega A$ are purely imaginary and often there is a diagonal transformation D such that

$$i\omega DAD^{-1} = \text{antisymmetric matrix}. \quad (\text{A18})$$

Then we can apply our arguments. As an example, we consider the wave equation, written as a first order system

$$\mathbf{u}_t = \begin{pmatrix} 0 & \epsilon^{-1} \\ 1 & 0 \end{pmatrix} \mathbf{u}_x. \quad (\text{A19})$$

The Fourier transform is of the form (A7).

Acoustic Equilibrium

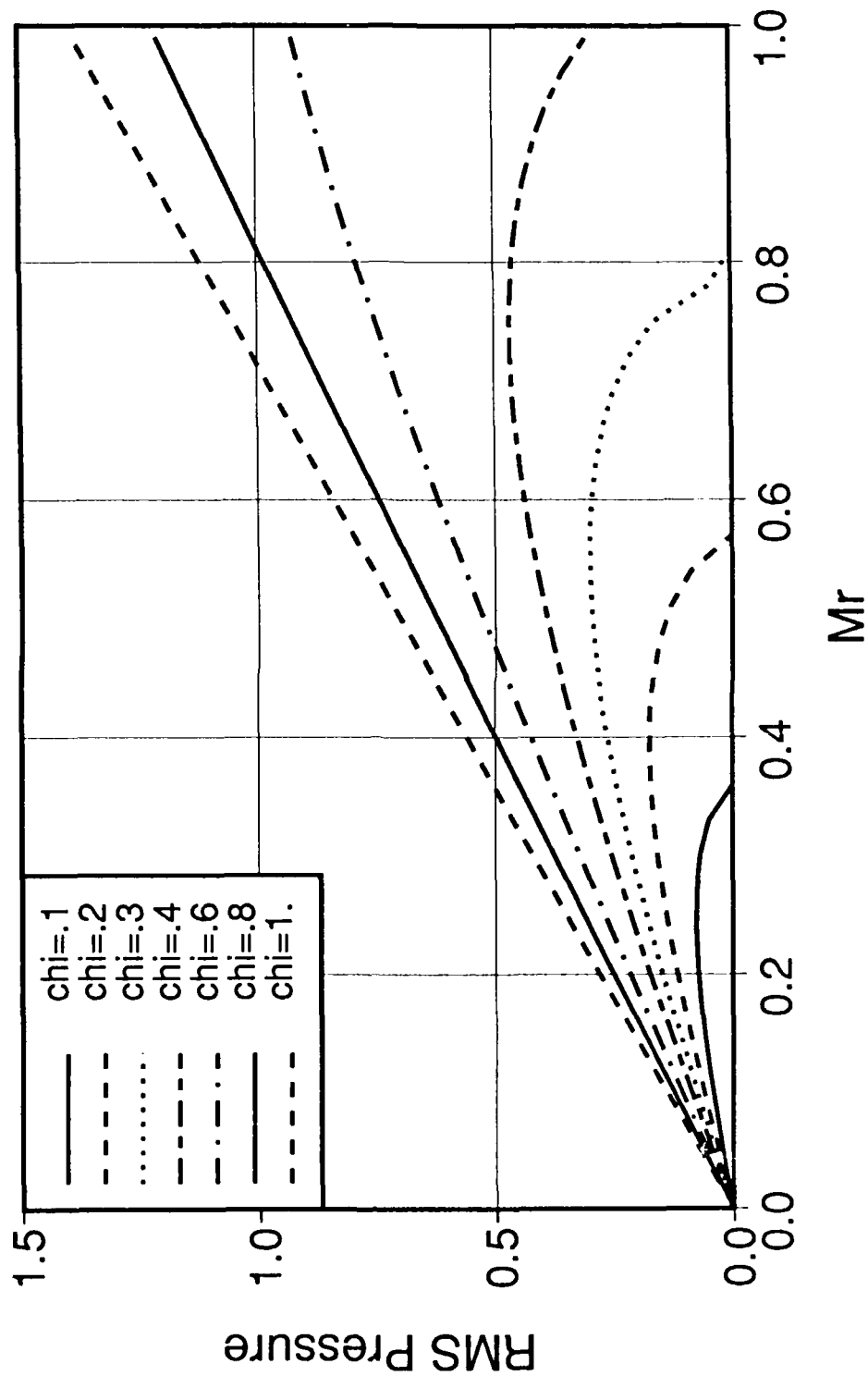


Figure 1: $\|p(M_R, \chi)\|$ as a function of M_R for different values of χ . The contour levels of χ all correspond to the condition that $F = 1$.



Report Documentation Page

1. Report No. NASA CR-181997 ICASE Report No. 90-15	2. Government Accession No.	3. Recipient's Catalog No.	
4. Title and Subtitle THE ANALYSIS AND SIMULATION OF COMPRESSIBLE TURBULENCE		5. Report Date February 1990	
		6. Performing Organization Code	
7. Author(s) Gordon Erlebacher M. Y. Hussaini H. O. Kreiss S. Sarkar		8. Performing Organization Report No. 90-15	
		10. Work Unit No. 505-90-21-01	
9. Performing Organization Name and Address Institute for Computer Applications in Science and Engineering Mail Stop 132C, NASA Langley Research Center Hampton, VA 23665-5225		11. Contract or Grant No. NAS1-18605	
		13. Type of Report and Period Covered Contractor Report	
12. Sponsoring Agency Name and Address National Aeronautics and Space Administration Langley Research Center Hampton, VA 23665-5225		14. Sponsoring Agency Code	
		15. Supplementary Notes Langley Technical Monitor: Richard W. Barnwell Submitted to Theoretical & Computational Fluid Dynamics Final Report	
16. Abstract This paper considers turbulent flows at low turbulent Mach numbers. Contrary to the general belief that such flows are almost incompressible, (i.e. the divergence of the velocity field remains small for all times), it is shown that even if the divergence of the initial velocity field is negligibly small, it can grow rapidly on a non-dimensional time scale which is the inverse of the fluctuating Mach number. An asymptotic theory which enables one to obtain a description of the flow in terms of its divergence-free and vorticity-free components has been developed to solve the initial-value problem. As a result, the various types of low Mach number turbulent regimes have been classified with respect to the initial conditions. Formulae are derived that accurately predict the level of compressibility after the initial transients have disappeared. These results are verified by extensive direct numerical simulations of isotropic turbulence.			
17. Key Words (Suggested by Author(s)) compressible turbulence, asymptotics, direct simulation		18. Distribution Statement 02 - Aerodynamics Unclassified - Unlimited	
19. Security Classif. (of this report) Unclassified	20. Security Classif. (of this page) Unclassified	21. No. of pages 29	22. Price A03